Density fingering in spatially bimodulated Hele-Shaw cells

Tamara Tóth, Dezső Horváth, Ágota Tóth *

Department of Physical Chemistry, University of Szeged, Rerrich Béla tér 1., Szeged, H-6720, Hungary

Abstract

Density fingering in the chlorite-tetrathionate reaction has been studied experimentally in Hele-Shaw cells with spatially modulated gapwidth. The periodic modulation parallel and perpendicular to the front propagation is introduced in the form of round depressions in the inner wall of the reaction vessel. Both the initial and the long time behavior have been studied while varying the chemical composition, the gapwidth, and the periodicity of the modulation. We have shown that although the initial pattern formation is unaffected, an enhanced tip splitting accompanies the general coarsening of the structures during the long time behavior.

* *Email address:* atoth@chem.u-szeged.hu

1 Introduction

A simple spatiotemporal pattern arising from the interaction of an autocatalytic reaction and transport processes is a propagating reaction-diffusion front[1]. In autocatalytic chemical reactions the reactants are converted into products in a thin zone defined as the front where the reactants and the products mix, and the diffusion of the autocatalyst molecules drives the front into the fresh reactant zone. When the density of solution changes in the course of the reaction, the system may become hydrodynamically unstable depending on the orientation with respect to the gravity field. If a solution layer with higher density develops on top, the buoyant forces give rise to convection rolls that distort the original shape of the reaction fronts, hence affect not only the velocity of front propagation due to the enhanced mixing of components[2,3] but also the evolution of spatial patterns[1,4].

Several experimental[5–8] and numerical studies [9–13] have been carried out in order to quantitatively describe the effect of convection in wide and narrow reaction vessels, so called Hele-Shaw cells[14]. Dispersion curves were introduced to characterize the initial pattern evolution where the growth rate is given as a function of its wave number. Positive growth rate expresses that the mode is convectively unstable and hence its amplitude increases exponentially with time, while a negative value represents a convectively stable mode, the contribution of which to the evolving pattern decreases with time. The long time behavior, generally characterized by the mixing length, have also been investigated both numerically[15,16] and experimentally[17–19] for these systems.

Some of the theoretical analyses[9,10,13] of these thin reactive layers use Darcy's law to estimate the velocity field for the fluid which was originally developed to describe fluid motion in a porous medium. Experimental efforts have therefore been made not only to show the validity range of Darcy's law but also to approach towards reaction fronts in genuine porous media. The first approximation of the varying channel size in natural porous media was the introduction of periodic spatial variation in the solution thickness.[20,21] This is a promising candidate since a theoretical work on viscous fingering has pointed out the importance of the imposed wavelength on the properties of the arising pattern in a periodically heterogeneous porous medium[22,23].

It has been proved experimentally that the heterogeneity has a significant contribution to the development of front patterns[20,21] in convective fingering where fluid motion arises because of density gradients. If the wave number of the imposed heterogeneity matches that of the structure appearing initially at constant solution thickness, resonance amplification can take place.[20] It has also been shown that the variation of chemical composition, solution thickness, and the periodicity of the spatial perturbation can lead to the development of three distinct structures: symmetric fingers with characteristic wavelength equal to or half of that associated with the modulation of gapwidth, and cellular patterns only in the thicker regions.[21]

An obvious continuation is the introduction of heterogeneity into the walls of the reaction chamber both perpendicularly and parallel to the direction of front propagation. For the experimental study we have selected the chlorite-tetrathionate reaction[24], which is an acid-catalyzed and highly exothermic reaction exhibiting a rich variety of spatiotemporal reaction-diffusion structures[25–27]. At room temperature the products are denser than the re-

actants therefore in thin solutions downward propagating planar fronts are hydrodynamically unstable and density fingering is going to lead to the formation of cellular structures. Upward propagating fronts can be either stable or unstable depending on the initial experimental conditions.

In this work we are going to characterize experimentally both the initial pattern evolution and the long time behavior of the finger development in the chlorite-tetrathionate reaction run in a special Hele-Shaw reaction vessel with bimodulated gapwidth. These experimental quantities can be employed for further theoretical investigations of density fingering in simple autocatalytic systems in porous media.

2 Experimental

We used reagent-grade chemicals (Sigma, Aldrich, Reanal) except for $NaClO_2$, which had been recrystallized twice as described earlier[28]. Besides the reactants, sodium hydroxide was added to eliminate self-initiation, while bromophenol blue indicator to visualize the reaction. To achieve appropriate wetting along the uneven surface, we also poured a small amount of sodium lauryl sulfate into the solution. The solutions, with compositions summarized in Table 1, were prepared at room temperature and injected into the reaction vessel. The Hele-Shaw cell consisted of two 8 mm thick Plexiglas walls and a 0.6–1 mm thick spacer. The appropriate nonuniformity was introduced in the form of 0.1 mm deep round depressions with a 3 mm or 6 mm diameter milled in the inner walls of the cell as shown in Fig. 1, corresponding to a periodic modulation with $\lambda = 6$ mm or 12 mm. Upon assembling the unit, the depressions are positioned in phase in the facing walls of the Hele-Shaw cell.

Planar fronts were initiated electrochemically by applying a 3 V potential difference between two parallel Pt wires (0.25 mm in diameter) for a few seconds. The traveling fronts were monitored by a monochrome CCD camera, and the frames were digitized in 2–10 s intervals. A cut-off filter (maximum transmission at 590±10 nm) between the camera and the cell was applied to enhance the contrast between the fresh (blue) and the reacted (yellow) solution.

The dispersion curves characterizing the initial evolution of the pattern formation were determined as described previously[6,7]. One-dimensional Fourier transformation was applied on the front profiles with a Hann window to determine the Fourier amplitudes, which exponentially grow or decay in the early stage of the front evolution. The growth rate of the given mode was therefore calculated for the dominant—first 30—Fourier modes as the slope of the initial linear time evolution of the logarithm of the Fourier amplitudes. Each dispersion curve is the result of averaging at least six experiments. For characterization of the long time behavior, the cell number was counted manually for each captured frame.

3 Results & Discussion

In our experimental conditions upward propagating planar fronts are stable while downward propagating fronts are unstable leading to cellular structures with a characteristic wavelength of 3–4 mm, since the products have larger density than the reactants. Figure 2 shows typical images of the downward propagating fronts in the special spatially bimodulated Hele-Shaw cells. Independently of the chemical composition and gapwidth applied, we have found

that cells with distinctly smaller amplitude and wavelength are imposed on the cellular structures typical for density fingering. The size of these small cells generally corresponds to the diameter of the depressions in the walls of the container. The observation of the temporal evolution (see Fig. 3) reveals that the initial fingering pattern resembles the structure developing in regular Hele-Shaw cells. The difference arises during the long time behavior, since besides the ever present merging enhanced continuous tip splitting occurs which is remarkably more significant and frequent than in regular reaction vessels. The phenomenon is found to be robust; by varying the physical conditions—such as gapwidth and the spatial periodicity of the heterogeneity—or the chemical composition, we do not observe any apparent change in the structure except the minor variation in the amplitudes.

In order to characterize the initial development of the unstable downward propagating fronts, we have constructed the dispersion curves corresponding to three different reaction vessels: a) a regular Hele-Shaw cell (with planar walls), b) a cell with spatial modulation perpendicular to the propagation of fronts[20,21], and c) the spatially bimodulated vessel with the setup shown in Fig. 1. The solid lines with squares in Fig. 4a illustrate the typical parabolic curve observed for convectively unstable fronts. The fastest growing mode has $k_m \approx 1.5$ mm^{-1}, which corresponds to an initial pattern with an average wavelength of 4 mm. When modulation perpendicular to the front propagation is introduced, the fronts become more unstable as we have described in earlier studies[20,21], therefore the fingers evolve faster resulting in greater growth rates (dotted line in Fig. 4a). Since the wavelength of the spatial modulation approximately matches the wavelength of the pattern evolving from fronts propagating in regular Hele-Shaw reaction vessels, resonance amplifi-

cation takes place at $k_m = 1.55$ mm^{-1}, i.e, the spatial modulation drives the initial pattern formation.[20] The scenario, however, is entirely different when spatial modulation parallel to the front propagation is also present. The curve belonging to the bimodulated system (dashed line) follows a parabola with a maximum at $k_m = 1.5$ mm^{-1}, very similarly to that of the regular case (solid line). This resemblance can be easily rationalized by inspecting the spatial variation of the gapwidth in the reaction vessel. In the first row of the circular depressions the fingering pattern is expected to be driven by the spatial modulation upon matching wave numbers, however, the next row of depressions is positioned with a $\lambda/2$ shift, leading to the total attenuation of the appropriate mode.

The similarity between the homogeneous and the bimodulated gapwidth is not restricted to the parameter range of resonance amplification. We may also choose conditions where the fingering pattern has the intriguing structure consisting of planar front segments in the thin sections and pairs of cells in the thicker sections of the container in the transverse modulation. For modulation with wavelength $\lambda = 12$ mm, it can be achieved by using a reactant solution with composition B in Table I,[21] in which case the initial pattern has a bimodal dispersion curve (dotted line in Fig. 4b) with two maxima at wave numbers of 1.2 mm^{-1} and 2.4 mm^{-1} in accordance with our earlier works[21]. The dispersion curve for the regular (solid line) and the bimodulated (dashed line) case is again described by a parabola with the most unstable mode at $k_m = 1.4$ mm^{-1} and $k_m = 1.6$ mm^{-1}, respectively. The latter scenario represents a hydrodynamically more unstable system as a result of the minor increase in the average gapwidth due to the spatial modulation.

To investigate the long time behavior we have monitored the front evolution.

In regular reaction vessels the cells—after the quick appearance of the cellular structure—continuously merge giving rise to a coarsening structure with continuously increasing wavelength and hence decreasing cell number in the observation window as illustrated with a solid line in Fig. 5. Although with the spatial heterogeneities introduced perpendicularly to the front propagation, the modulation drives the initial evolution of fingering patterns, at the later stages the nonlinear interactions of the cells become dominant and the merging of cells is exhibited giving rise to similar behavior (see dashed line in Fig. 5) to that observed with regular Hele-Shaw vessels. Opposite scenario occurs with the addition of the second spatial modulation—parallel to the front propagation—in which case the continuous splitting of fingers becomes dominant and therefore the cell number in the observation windows settles to a greater value with respect to those in the regular and transverse modulated Hele-Shaw vessels.

In conclusion, we have shown experimentally that the bimodulation of gapwidth has no significant contribution to the initial development of cellular structures in density fingering of an autocatalytic system. The long time behavior is, however, considerably affected because of the enhanced continuous splitting of cells at the heterogeneities in contrast to the general coarsening leading to patterns with larger wavelength and amplitude observed either in regular Hele-Shaw cells or in cells with the spatially modulated gapwidth perpendicular to the front propagation.

Therefore the enhancement of the splitting of cells is due to the presence of the heterogeneity introduced to the system parallel to the front propagation. Furthermore this phenomenon is a general feature in fingering arising from either density difference or viscosity change. The patterns, however, are distinctly

different since for viscous fingering very thin and long fingers are splitting continuously.[23] It would also be interesting to analyze how the structure varies when the modulation of gap width is different in the two directions.

Acknowledgements

This work was financially supported by the Hungarian Research Fund (OTKA K72365) and ESA (C98036).

References

[1] I.R. Epstein, J.A. Pojman, An Introduction to Nonlinear Dynamics: Oscillations, Waves, Patterns, and Chaos, Oxford University Press, Oxford, 1998.

[2] I. Nagypál, Gy. Bazsa, I.R. Epstein, J. Am. Chem. Soc. 108 (1986) 3635.

[3] J.A. Pojman, I.R. Epstein, T.J. McManus, K. Showalter, J. Phys. Chem. 95 (1991) 1299.

[4] J.A. Pojman, A. Komlósi, I.P. Nagy, J. Phys. Chem. 100 (1996) 16209.

[5] M. Böckmann and S. C. Müller, Phys. Rev. Lett. 85 (2000) 2506.

[6] T. Bánsági, Jr., D. Horváth, Á. Tóth, J. Yang, S. Kalliadasis, A. De Wit, Phys. Rev. E 68 (2003) 055301.

[7] T. Bánsági, Jr., D. Horváth, Á. Tóth, Chem. Phys. Lett. 384 (2004) 153.

[8] L. Sebestiková, J.D. D'Hernoncourt, M.J.B. Hauser, S.C. Müller, A. De Wit, Phys. Rev. E 75 (2007) 026309.

[9] A. De Wit, Phys. Rev. Lett. 87 (2001) 054502.

[10] J. Yang, A. D'Onofrio, S. Kalliadasis, A. De Wit, J. Chem. Phys. 117 (2002) 9395.

[11] J. Martin, N. Rakotomalala, D. Salin, M. Böckmann, Phys. Rev. E 65 (2002) 051605.

[12] D.I. Coroian, D.A. Vasquez, J. Chem. Phys. 119 (2003) 3354.

[13] J. D'Hernoncourt, A. Zebib, A. De Wit, Chaos 17 (2007) 013109.

[14] H.S. Hele-Shaw, Nature 58 (1898) 34.

[15] A. De Wit, Phys. Fluids 16 (2004) 163.

[16] D. Lima, A. D'Onofrio, A. De Wit, J. Chem. Phys. 124 (2006) 014509.

[17] T. Bánsági, Jr., D. Horváth, Á. Tóth, J. Chem. Phys. 121 (2004) 11912.

[18] M. Böckmann, S. C. Müller, Phys. Rev. E 70 (2004) 046302.

[19] T. Rica, D. Horváth, Á. Tóth, Chem. Phys. Lett. 408 (2005) 422.

[20] D. Horváth, S. Tóth, Á. Tóth, Phys. Rev. Lett. 97 (2006) 194501.

[21] T. Tóth, D. Horváth, Á. Tóth, J. Chem. Phys. 127 (2007) 234506.

[22] A. De Wit, G.M. Homsy, J. Chem. Phys. 107 (1997) 9609.

[23] A. De Wit, G.M. Homsy, J. Chem. Phys. 107 (1997) 9619.

[24] L. Szirovicza, I. Nagypál, E. Boga, J. Am. Chem. Soc. 111 (1989) 2842.

[25] Á. Tóth, I. Lagzi, D. Horváth, J. Phys. Chem. 100 (1996) 14837.

[26] Á. Tóth, B. Veisz, D. Horváth, J. Phys. Chem. A 102 (1998) 5157.

[27] I. Szalai, F. Gauffre, V. Labrot, J. Boissonade, P. De Kepper, J. Phys. Chem. A 109 (2005) 7843.

[28] Á. Tóth, D. Horváth, A. Siska, J. Chem. Soc., Faraday Trans. 93 (1997) 73.

Table 1

Composition of the reactant solutions

	A	B
$[K_2S_4O_6]$/mM	3.75	5.00
$[NaClO_2]$/mM	15	20
[NaOH]/mM	1	1
[Bromophenol blue]/mM	8×10^{-2}	8×10^{-2}
[Sodium lauryl sulfate]/mM	3.33×10^{-3}	3.33×10^{-3}

Figure captions

Fig. 1 Scheme of the Hele-Shaw cell.

Fig. 2 Images of fronts for solution composition A in Table 1 with 1 mm gapwidth and $\lambda = 6$ mm (a), and for composition B in Table 1 with 0.6 mm gapwidth and $\lambda = 12$ mm (b). Lighter regions represent the denser product solution and darker ones the reactant. Field of view is 15 cm $\times$ 5.6 cm.

Fig. 3 Front evolution at 10 s intervals with experimental conditions corresponding to Fig. 2(a).

Fig. 4 Dispersion curves for downward propagating fronts for solution composition A in Table 1 with 1 mm gapwidth and $\lambda = 6$ mm (a), and for composition B in Table 1 with 0.6 mm gapwidth and $\lambda = 12$ mm (b). The solid line illustrates the dispersion curve for the vessel with no modulation, the dotted line that for the vertically modulated and the dashed line that for the bimodulated cell.

Fig. 5 The numbers of the cells in the evolving patterns as a function of time with experimental conditions corresponding to Fig. 2(a). The solid line corresponds to the vessel with no modulation, the dotted line to the vertically modulated and the dashed line to the bimodulated cell.

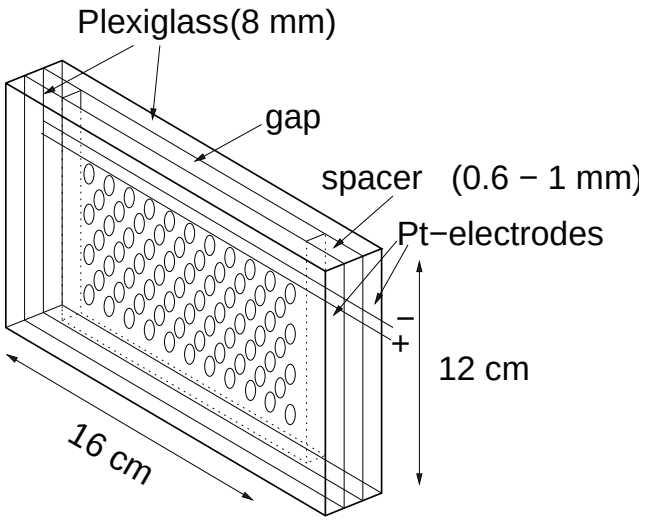

Fig. 1. T. Tóth ... Chem. Phys. Lett.

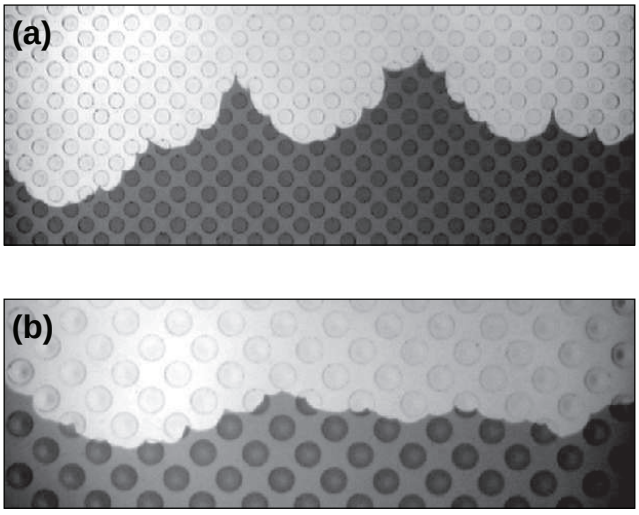

Fig. 2. T. Tóth ... Chem. Phys. Lett.

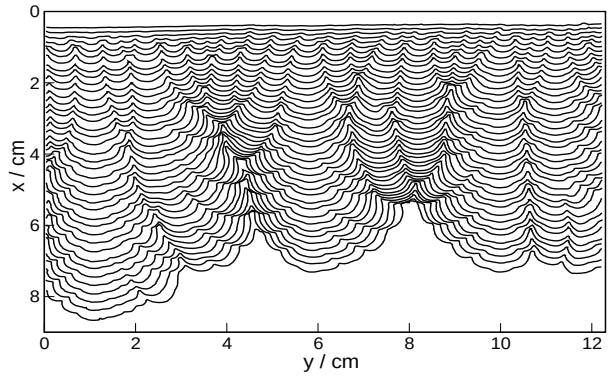

Fig. 3. T. Tóth ... Chem. Phys. Lett.

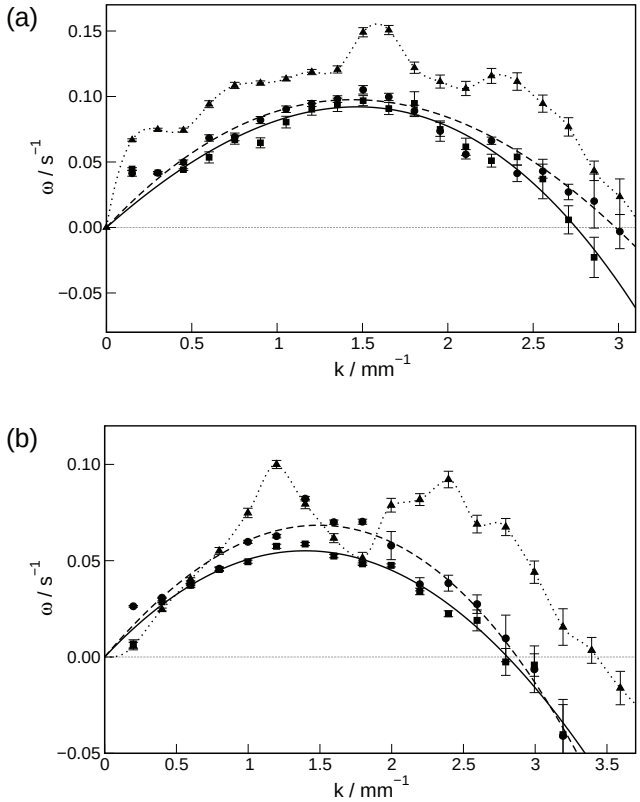

Fig. 4. T. Tóth ... Chem. Phys. Lett.

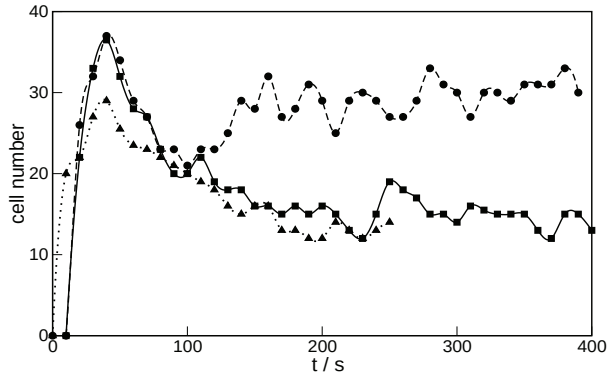

Fig. 5. T. Tóth ... Chem. Phys. Lett.

Graphical abstract for Chemical Physics Letters

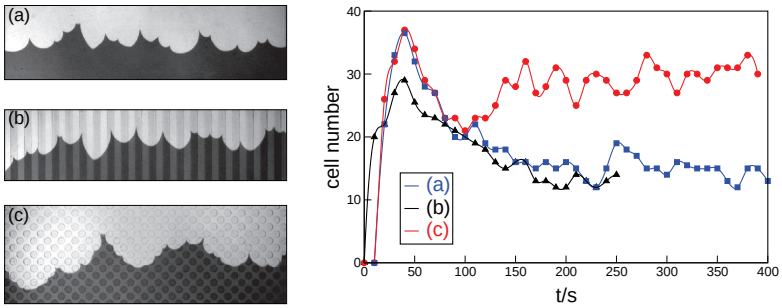

Enhanced tip splitting accompanying cell merging lead to patterns with significantly greater cell number in spatially bimodulated Hele-Shaw vessels.

*** Graphical Abstract (synopsis)**

Enhanced tip splitting accompanying cell merging lead to patterns with significantly greater cell number in spatially bimodulated Hele-Shaw vessels.